Performance Analysis of a Compact Eye-Shaped Slot Antenna for MIMO UWB Applications

RajiniAuthivel Rajendran[1], Vijayalakshmi Alagarsamy[2], Ebenezer Abishek[3], Mary Livinsa Z[4]

[1]Professor, Department of Electronics and Communication Engineering, Sri Sairam Engineering College and Research Scholar, VELS Institute of Science, Technology and Advanced Studies.
[2]Professor, Department of Electronics and Communication Engineering, VELS Institute of Science, Technology and Advanced Studies,Chennai-600117, India, Email: vijayalakshmi.se@velsuniv.ac.in
[3]Associate Professor, Department of Electronics and Communication Engineering, KCG College of Technology, Chennai-600097, India
[4] Associate Professor, Department of Electronics and Communication Engineering, VELS Institute of Science, Technology and Advanced Studies, Chennai-600117, India

Received: 05.04.2024 Revised : 14.05.2024 Accepted: 20.05.2024

ABSTRACT
This research paper introduces a compact multiple-input, multiple-output (MIMO) ultra-wideband (UWB) antenna design featuring an eye-shaped slot configuration. The proposed antenna structure comprises two eye-shaped slots positioned on a ground plane, with the strategic insertion of a T-shaped stub to enhance their isolation. The antenna exhibits an impressive impedance bandwidth spanning 3.5 GHz (4.83 to 8.35 GHz) while maintaining a compact footprint of 18.36 mm^2. Throughout the operational bandwidth, the mutual coupling between the two slots remains consistently below 20 dB. The research encompasses comprehensive modeling, manufacturing, and rigorous performance assessment through simulation and experimentation. The results validate the antenna's capabilities, demonstrating favorable radiation patterns, a low envelope correlation coefficient (ECC), and a substantial diversity gain. These attributes position the antenna as a promising candidate for integration into portable UWB devices, particularly as a sensor component, thus expanding its utility in wireless communication and sensing applications.

Keywords: slot, Microstrip, MIMO, planar, UWB.

I. INTRODUCTION

In 2002, the Federal Communications Commission (FCC) made a pivotal decision by allocating the 3.1-10.6 GHz band for Ultra-Wideband (UWB) applications. Alongside this allocation, the FCC recommended stringent power limits, with UWB devices operating in the 4.83-8.35 GHz frequency band requiring power levels to be maintained below 41.3 dBm/MHz [1]. In recent years, there has been a significant increase in interest surrounding the design and development of UWB antennas. This surge can be attributed to a pivotal move that opened up new possibilities for researchers and industries to explore the realm of UWB applications. The exploration and publication of UWB antenna designs have gained significant momentum due to the fundamental and integral role that antennas play in communication systems.

The challenges encountered by researchers and scientists engaged in UWB antenna design encompassed the pursuit of high data rates, robust security measures, cost-effectiveness, and minimal power consumption. There was also the problem of reliability and multipath fading in ultra-wideband (UWB) systems. One promising approach to overcoming these difficulties is to employ ultra-wideband (UWB) systems in tandem with the Multiple Input Multiple Output (MIMO) technology. MIMO systems possess the potential to enhance channel capacity while concurrently improving reliability and mitigating multipath fading. In MIMO systems, antennas must incorporate uncorrelated multiple radiating elements for efficient signal transmission and reception. These MIMO systems employ N*N elements at both the transmitter and receiver ends [2-4].

Achieving an ideally infinite level of isolation between antenna ports is a primary challenge when designing suitable antennas for MIMO applications. The minimum acceptable isolation level among ports is typically set at 15 dB. Various techniques have been employed to attain this level, including diversity polarization, neutralization lines, parasitic structures, Defective Ground Structures (DGS), metallic barriers, and periodic resonant structures [5-8].

In this particularly noteworthy instance, a two-element MIMO antenna that was tailored to the C and X bands was developed. By incorporating DGS, the antenna successfully achieved a remarkable level of isolation, reaching nearly 30 dB [9]. Similarly, in another study, an innovative U-shaped structure positioned between a pair of F-shaped radiators delivered inter-port isolation exceeding 30 dB for dual-band WLAN MIMO applications [10]. Further research in this domain revealed that arranging compact UWB MIMO antennas orthogonally and introducing fork-shaped slots in the ground plane yielded over 30 dB of isolation among the ports [11]. Novel and inventive UWB antennas, both with and without notch filters, were fabricated and evaluated for UWB MIMO applications [12–19], while a variety of MIMO antenna types were explored in [20–29].

A compact ultra-wideband fractal antenna, specifically designed for breast cancer detection applications, is one example of the innovative approaches being explored in UWB antenna design. The potential of compact UWB antennas in medical diagnostics is demonstrated, highlighting their versatility and effectiveness in diverse applications [30]. Similarly, advancements in compact UWB antenna technology are exemplified by a compact diamond-shaped ultra-wideband antenna system for diagnosing breast cancer, further emphasizing the critical role of antenna design in modern communication and diagnostic systems [31].Moreover, the exploration of innovative antenna designs continues with the development of specialized antennas for maritime applications, such as the WSN-based maritime border alert system, which underscores the importance of compact and efficient antenna systems in challenging environments [32].

An interesting cross-polarized four-port dual-band MIMO antenna array was proposed in [33], and in [34], a compact printed planar eye-shaped dipole antenna catered to Ultra-Wideband wireless applications. A slit slot between antenna units and rectangular openings was introduced in [35] to achieve high isolation. In [36], the single antenna was replicated and grouped in an orthogonal pattern to design a multi-port antenna to attain high isolation. This article not only presents a comprehensive design procedure but also offers a thorough analysis of the performance of the proposed UWB MIMO antenna functioning at a resonating frequency of 6 GHz and catering to diverse communication systems.

II. ANTENNA DESIGN

The antenna design in this study revolves around a two-element configuration, featuring circular radiating elements with ellipsoidal slots. This design is tailored for operation within the Ultra-Wideband (UWB) frequency range, spanning from 3.1 to 10.6 GHz. While the proposed structure is straightforward and widely employed, it adequately covers the requisite frequency band. It is important to note that this configuration may not be the most optimized choice for applications necessitating Gaussian impulse shaping filters, commonly encountered in UWB radio systems.

Figure 1 illustrates the geometric layout of the proposed antenna design. The antenna is constructed using FR4 as the dielectric substrate material, chosen for its desirable electrical properties. The selected substrate is FR4, with a thickness of 1.6 mm and a relative permittivity (ε_r) of 4.4. Furthermore, it exhibits a dielectric loss tangent (tan δ) of 0.02, a crucial parameter to assess the antenna's efficiency and performance. The antenna structure boasts compact dimensions, measuring 18 × 36 mm^2, ensuring optimal space utilization without compromising on performance. The radiating element takes the form of a circular patch with a radius of 4.4 mm. In this design, an elliptical slot is introduced, characterized by a major axis measuring 5.3 mm and a minor axis measuring 3.8 mm. This elliptical slot serves the dual purpose of enhancing bandwidth and maintaining a compact overall size.

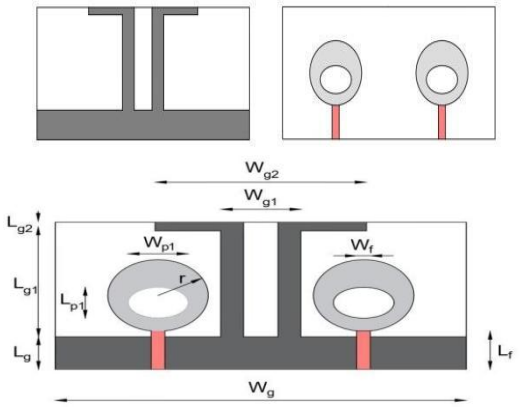

Fig 1. Antenna Geometry: Front and Back View

According to Balanis (1982), the actual radius of the circular radiating patch is as follows:

$$r = \frac{F}{\left\{1+\frac{2h}{\pi\varepsilon_r F}\left[\ln\left(\frac{\pi F}{2h}\right)+1.7726\right]\right\}^{\frac{1}{2}}} \quad (1) \qquad \text{where } F = \frac{8.791X10^9}{f_r\sqrt{\varepsilon_r}} \quad (2)$$

Each radiator is fed through a 50-ohm microstrip feed line positioned along the lower edge of the radiator. To enhance antenna performance, a rectangular ground plane is situated beneath the feed line. By combining horizontal and vertical strips, an extruding stub is another modification to the ground plane. This modification significantly improves the isolation factor between the radiating elements, resulting in an effective decoupling structure.

The development of the patched antenna involves the design of a single radiator with a resonant frequency of fr = 6 GHz and a height of h = 1.6 mm. The radius of the patch is determined to be 5.775 mm using equation (1), and the corresponding value of F is calculated to be 6.984 mm using equation (2). The dimensions of the substrate are hypothesized to be equal to twice the diameter of the patch, denoted as Ls = Ws = 2*2r = 23.1 mm. The simulation of the single radiator and multiple-input multiple-output (MIMO) antenna was conducted, and the performance of the S_{11} parameter was analyzed. A parameter sweep was conducted on the radius of the patch due to the deviation of the resonant frequency of the designed antenna from the specified value and the simulation result is presented in Figure 2. A resonant frequency of 6 GHz was obtained for a radius (r) of 4.4 mm.

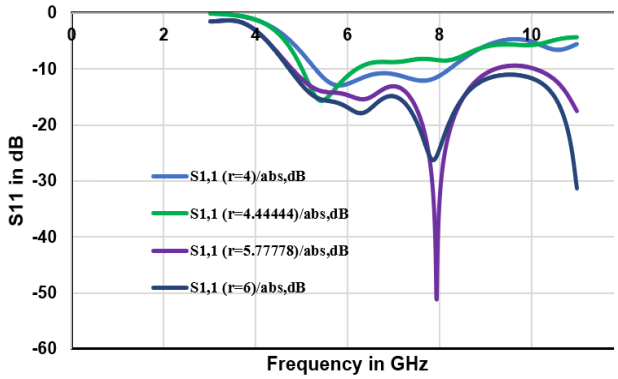

Fig 2. Parameter sweep on the radius of the patch before optimization.

The dimensions and position of the slot were subsequently optimized. The simulated result obtained is shown in Figure 3.

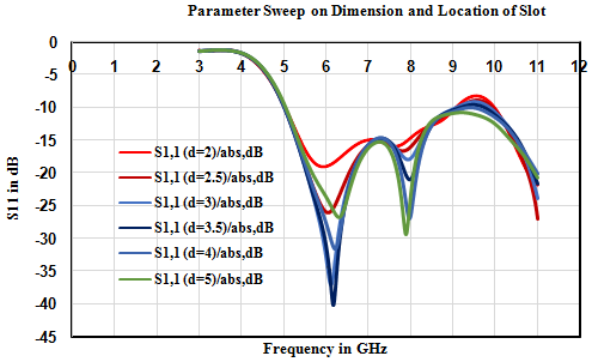

Fig 3. Parameter sweep on the dimensions and location of the slot.

The Trust Region Framework Algorithm is employed to determine the optimal parameters for the length (L_s) and width (W_s) of the antenna, as well as the dimensions of the major (W_{p1}) and minor (L_{p1}) axes of the slot. The positioning of the slot relative to the bottom of the patch has been optimized to ensure optimal performance as per the requirements.

The screen shot of the optimizer is shown in figure 4. 'b' corresponds to $W_{p1}/2$'c'corresponds to $Lp_1/2$. 'd' is the position of the slot from the bottom of the circular patch. The physical dimensions of the antenna after optimization are given in Table 1.

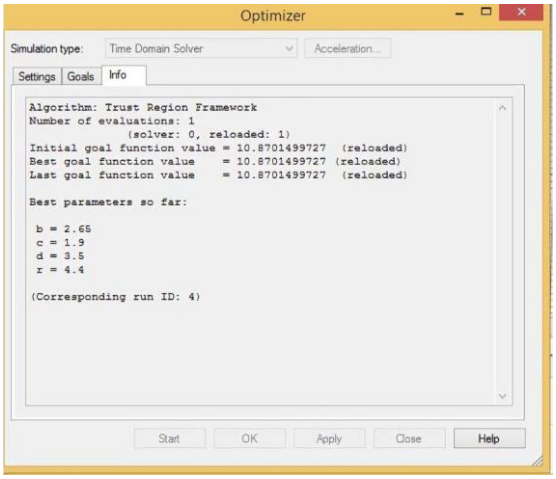

Fig 4. Determined Optimal Parameters

Table 1. Physical dimensions of the proposed antenna

Parameters	Value (mm)
Wg	36
Lp1	3.8
Wp1	5.3
Wf	1.2
Lf	4.64
r	4.4
Lg1	12.5
Wg1	7
Wg2	18.5
Lg2	1
Lg	4.5

The performance of the antenna was simulated in a great deal of detail by making use of the numerical technique known as Finite Difference Time Domain (FDTD) within the environment known as CST Studio Suite.

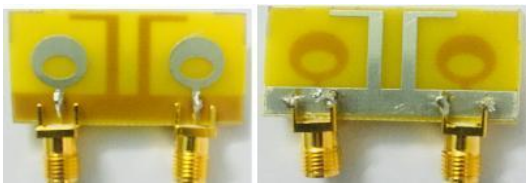

Fig 5. Front and rear perspectives of the developed antenna.

Figure 5 shows the front and back views of the antennas, respectively. SMA connectors are used to excite the radiating elements.

III. RESULT AND DISCUSSION

The results of our comprehensive analysis of a compact eye-shaped slot antenna designed for MIMO UWB applications are presented in this section.

The simulated results, illustrated in Figure 6, reveal a resonating frequency of 6.13 GHz. More importantly, the antenna's impedance bandwidth spans from 4.82 GHz to 8.35 GHz, effectively covering the entire UWB frequency band. This wide bandwidth is crucial for accommodating the diverse frequency range of UWB. applications.

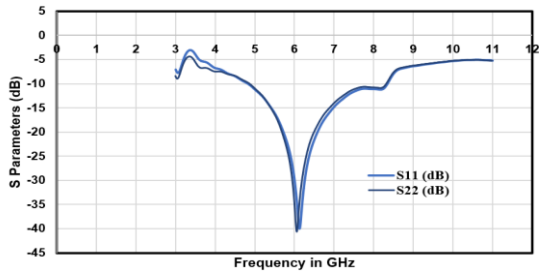

Fig 6. Proposed Antenna Port 1 and Port 2 Reflection Coefficient vs. Frequency

Figures 7a and 7b showcase the transmission coefficient plots at ports 1 and 2. Within the operational frequency band, the transmission coefficient consistently measures below -25 dB. This observation signifies excellent isolation between the two ports, a vital characteristic for MIMO antenna systems, as it minimizes interference between antenna elements.

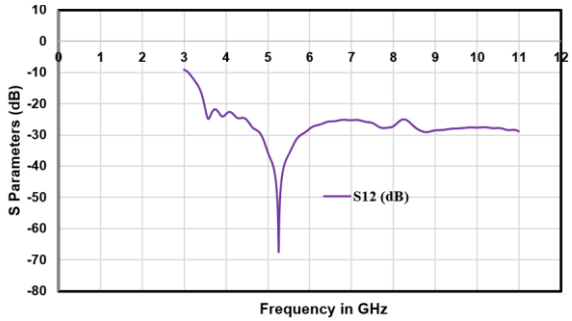

Fig 7a. Proposed Antenna Port 1 Transmission Coefficient vs. Frequency

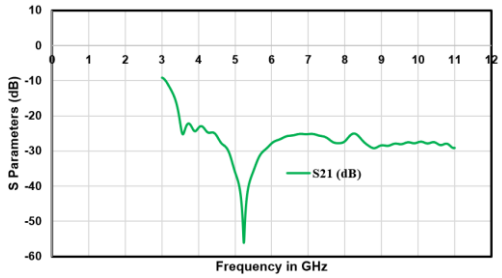

Fig 7b. Proposed Antenna Port 1 Transmission Coefficient vs. Frequency

The relationship between frequency and the voltage standing wave ratio (VSWR) is depicted here in Figure 8. Remarkably, the VSWR for the radiating element remains below 2 within the specified frequency band. This adherence to design requirements ensures efficient power transfer and impedance matching, enhancing antenna performance.

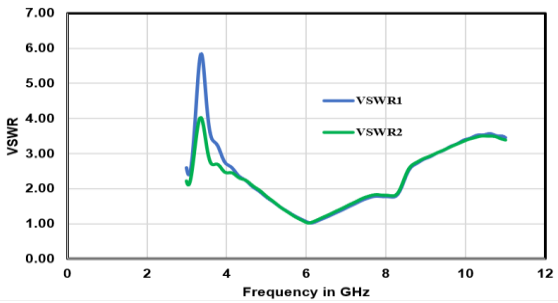

Fig 8. VSWR vs. frequency plot of the proposed antenna.

The three-dimensional radiation pattern of the antenna at 6 GHz is depicted in Figure 9. The proposed antenna has a maximum gain of 3.05 dBi when it is fully operational. The radiation pattern is omnidirectional in the E-plane and has a beamwidth of around 80 degrees in the H-plane.

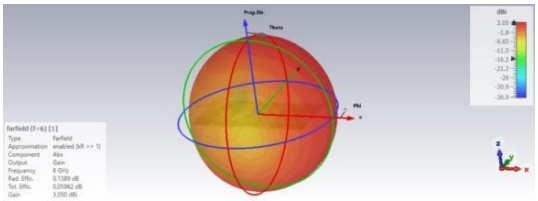

Fig 9. Three-dimensional far-field polar pattern of the proposed antenna.

Figures 10a and 10b, respectively, illustrate the surface current distributions that are present at port 1 and port 2, respectively. The obtained distributions provide confirmation of the successful isolation achieved in the antenna design. Additionally, they validate that the antenna is symmetrically excited at both ports, which is crucial for maintaining consistent radiation patterns.

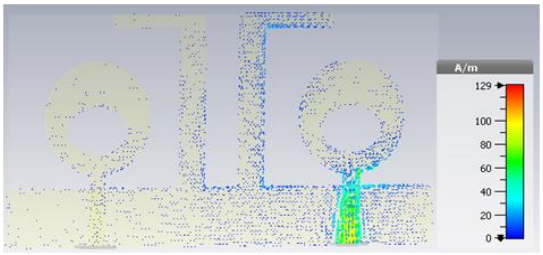

surface current (f=6) [1]	
Type	H-Field
Frequency	6 GHz
Phase	0
Maximum	129.285 A/m
Max. position	29.350, 5.640, 0.600

Fig 10a. Proposed antenna Port 1 Surface Current Distribution.

surface current (f=6) [2]	
Type	H-Field
Frequency	6 GHz
Phase	0
Maximum	127.402 A/m
Max. position	6.650, 5.640, 0.600

Fig 10b. Proposed antenna Port 2 Surface Current Distribution.

Fig 11. Experimental Setup Utilized for Conducting the Testing of the Proposed Antenna.

Throughout the testing procedure for the antenna we developed, a Vector Network Analyzer (Anritsu MS2038C VNA Master) was utilized. The apparatus that was utilized in the testing of the antenna is depicted in Figure 11.

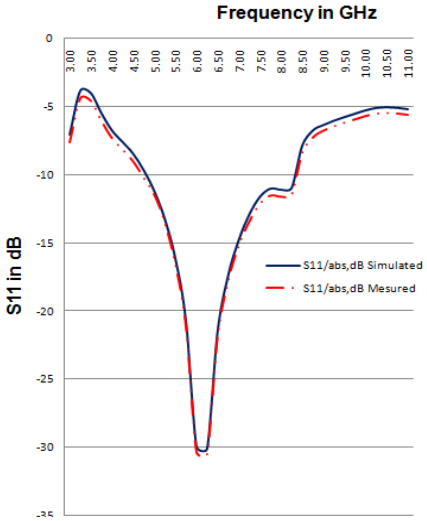

Fig 12(i). Reflection coefficient (S11) versus frequency plot for the proposed antenna, measured and simulated.

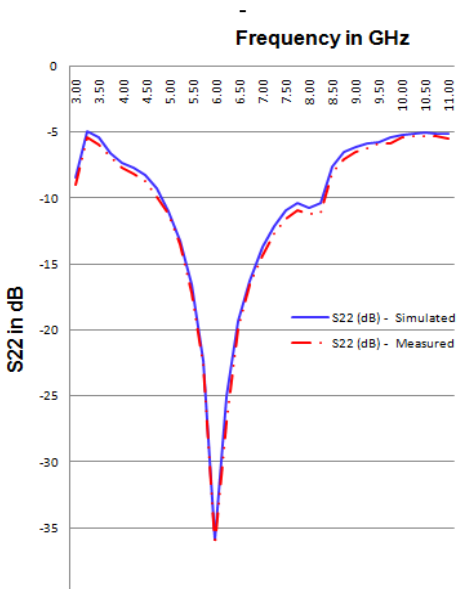

Fig 12(ii). Reflection coefficient (S22) versus frequency plot for the proposed antenna, measured and simulated.

Figure 12(i) and 12(ii) displays the measured reflection coefficient characteristics of the antenna. The reflection coefficient plot exhibits remarkable congruence between the simulated and measured outcomes. This close alignment between simulation and measurement results underscores the validity and accuracy of our antenna design and modeling approach.

We carried out measurements of the radiation pattern inside an anechoic chamber in order to further validate the performance of the proposed antenna design that we developed. The test setup used a Verdant JR12 horn antenna as the transmitting antenna. The validation was conducted at 6 GHz, which is important for our wireless MIMO UWB applications. Figures 13 to 16 compare the measured and simulated radiation patterns of the proposed antenna in the E and H principal planes for ports 1 and 2. The measurements indicate that the simulated and measured results are consistent, which demonstrates that the antenna is appropriate for the intended application. However, it is worth noting that minor inconsistencies in the results were observed, attributed to fabrication tolerances.

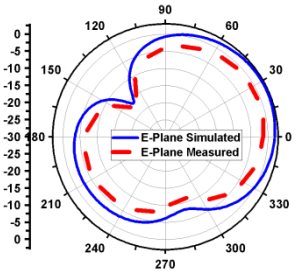

Fig 13. E Plane Radiation Patterns for Port 1 of the Proposed Antenna, Measured and Simulated.

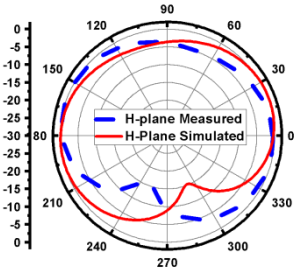

Fig 14. H-Plane Radiation Patterns for Port 1 of the Proposed Antenna, Measured and Simulated.

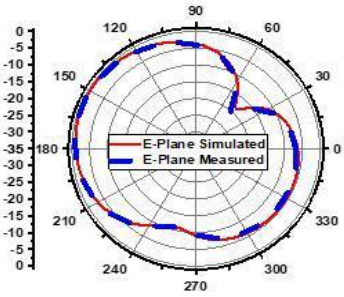

Fig 15. E-Plane Radiation Patterns for Port 2 of the Proposed Antenna, Measured and Simulated.

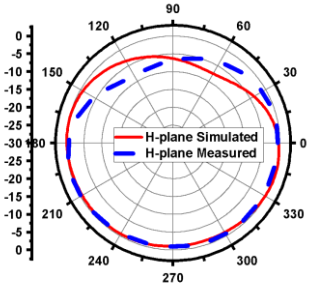

Fig 16. H-Plane Radiation Patterns for Port 2 of the Proposed Antenna, Measured and Simulated.

Beyond the antenna's individual characteristics, we have evaluated its MIMO performance, a critical consideration in modern wireless communication systems.

The investigation uses the Envelope Correlation Coefficient (ECC) to measure the correlation between the two antenna elements. Figures 17. (i) and (ii) demonstrate that the ECC remains below 0.5, indicating an effective lack of correlation among the antenna elements across all frequencies. This property is highly desirable for MIMO systems, as it maximizes diversity gain and enhances communication reliability. This parameter of the MIMO antenna is evaluated from the S parameter using the expression

$$ECC = \frac{\left|S_{ii}^{*}S_{ij}+S_{ji}^{*}S_{jj}\right|^{2}}{\left(1-|S_{ii}|^{2}-|S_{ij}|^{2}\right)\left(1-|S_{ji}|^{2}-|S_{jj}|^{2}\right)} \quad (5)$$

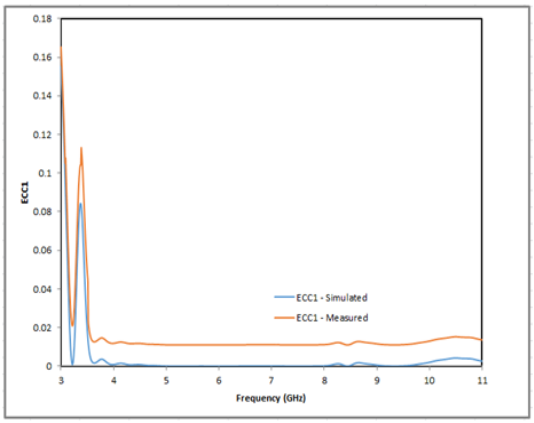

Fig 17. (i) Envelope correlation plot at port 1

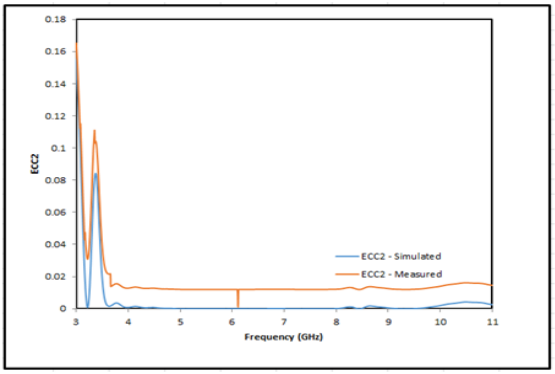

Fig 17. (ii) Envelope correlation plot at port 2

We found that a 2-element MIMO antenna with an error correction coding (ECC) value of 0 has a diversity gain (DG) of 10 dB. This value is considered ideal as it signifies a higher level of reliability for the communication link. Due to the finite value of ECC, the diversity gain is reduced by a factor of $\sqrt{1-\mathrm{ECC}^2}$. Hence, the expression for directive gain is

$$\mathrm{DG} = 10 * \sqrt{1-\mathrm{ECC}^2} \qquad (6)$$

The calculations conducted indicate that the antenna possesses a DG (directivity gain) ranging from 9.9 to 10 throughout the entire frequency range. This finding suggests that the antenna has the potential to greatly enhance the dependability of communication links. This metric emphasizes the antenna's effectiveness in real-world MIMO applications.

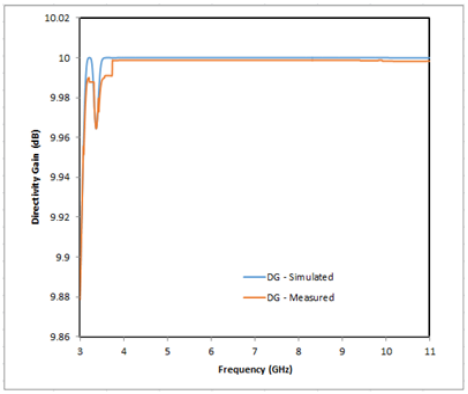

Fig 17. (iii) Directive gain of the antenna

The difference in the amount of radiated power that the various antenna elements produce is another crucial factor in MIMO systems. The value is quantified using the ratio of power in the two antennas.

$$\mathrm{k} = \min\left(\frac{\mathrm{MEG}_1}{\mathrm{MEG}_2}, \frac{\mathrm{MEG}_2}{\mathrm{MEG}_1}\right) \qquad (7)$$

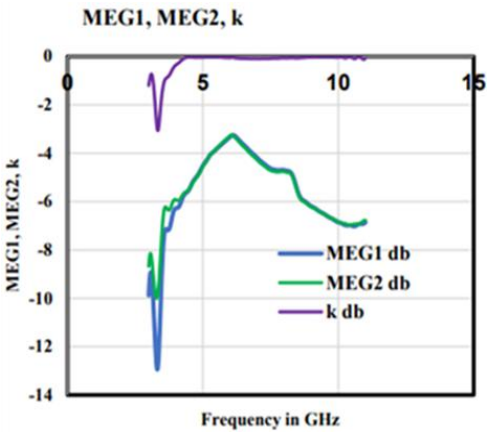

Fig 17. (iv) MEG_1, MEG_2 and Power Ratio of the proposed antenna.

The Channel Capacity Loss (CCL) parameter, which is a crucial component of MIMO systems, measures the potential capacity for data transmission. The achieved CCL of our antenna is less than 0.4 bits/sec/Hz, which is similar to the performance of other MIMO antennas discussed in existing literature. This result highlights the robust data transmission capabilities of our antenna. The expression to calculate CCL is as follows:

$$CCL = -\log_2 \det R \quad (9a)$$

where R is the correlation matrix of the two-port MIMO system at the receiver terminal.

$$R = \begin{pmatrix} \rho_{11} & \rho_{12} \\ \rho_{21} & \rho_{22} \end{pmatrix} \quad (9b)$$

$$\rho_{11} = (1 - |S_{11}|^2 - |S_{12}|^2) \quad (10)$$

$$\rho_{22} = (1 - |S_{22}|^2 - |S_{21}|^2) \quad (11)$$

$$\rho_{12} = -(S_{11}^* S_{12} + S_{21}^* S_{12}) \quad (12)$$

$$\rho_{21} = -(S_{22}^* S_{21} + S_{12}^* S_{21}) \quad (13)$$

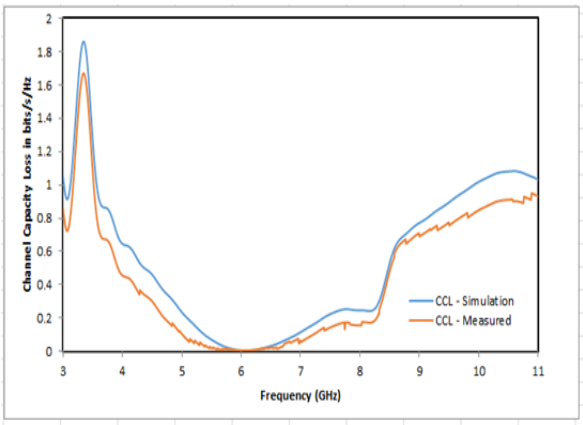

Fig 17. (v) Channel Capacity Loss of the proposed antenna.

Within the scope of this investigation, we delved into the concept of the Total Active Reflection Coefficient (TARC) and its importance in elucidating the power characteristics of N-port microwave components.

$$TARC = \sqrt{\frac{\sum_{i=1}^{N} (b_i)^2}{\sum_{i=1}^{N} (a_i)^2}} \quad (14)$$

The variables "a_i" and "b_i" denote incident power and reflected power, respectively, within the context of our analysis. The Total Available Received Power (TARC) can be mathematically formulated in relation to the S-parameters.

$$TARC = \sqrt{\frac{(|S_{11} + S_{12} e^{j\varphi}|)^2 + (|S_{21} + S_{22} e^{j\varphi}|)^2}{2}} \quad (15)$$

In a MIMO system, the phase difference between the excitations of each antenna is denoted by φ.

Figure 17(vi) given below is a representation of the TARC performance, which measures the return loss of the antenna.The proposed antenna has a TARC that is lower than -2, which is indicative of its high level of performance and its suitability for practical application.

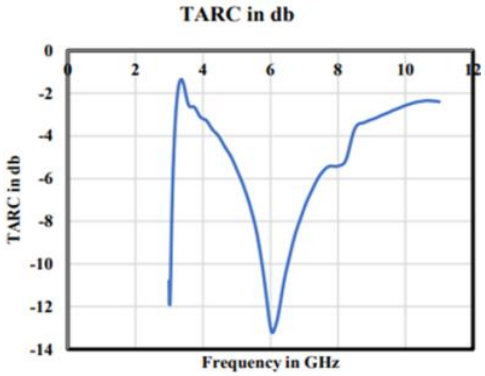

Fig 17. (vi) TARC performance of the proposed antenna.

The proposed compact multiple-input, multiple-output (MIMO) ultra-wideband (UWB) antenna design stands out for its impressive impedance bandwidth spanning 3.5 GHz (4.83 to 8.35 GHz) while maintaining a compact footprint of 18.36 mm^2. Strategic insertion of a T-shaped stub enhances isolation between eye-shaped slots, ensuring consistently low mutual coupling below 20 dB throughout the operational bandwidth. Comprehensive modeling and rigorous performance assessment validate the antenna's capabilities, including effective isolation, symmetrical excitation, and diversity gain ranging from 9.9 to 10 dB, highlighting its potential for enhancing communication reliability in MIMO systems. Moreover, the antenna's low Channel Capacity Loss (CCL) of less than 0.4 bits/sec/Hz underscores its robust data transmission capabilities crucial for efficient communication in modern wireless systems.
Table 2 provides a comparison between the radiation characteristic parameters of this work and those of recent related research works.

Table 2. Comparison between the earlier studies in the literature and proposed antenna.

Antenna	Antenna Size mm^2	Frequency range (GHz)	Method	Isolation (dB)	ECC	CCL Bit/s/Hz	Gain dBi
[20]	18 X 28	1.9-14	Stubs	<-20	<0.09	<0.04	0.4-4.8
[21]	40 X 60	2.5-11.0	Stub	<-20	<0.019	-	2-7.4
[22]	35 X 50	3.0-11.0	DGS	<-25	<0.004	-	3
[23]	31 X 26	2.8-12.0	Linked Stub	<-25	<0.001	-	<5
[24] (Antenna 3)	38 X 28	-	-	<-15	-	-	-
[37]	68 X 40	3.1-10.6	Stub	<-15	<0.01	-	<2.5
[38]	58.6 X 46	3.1-10.6	Shorting Strip	<-13	<0.02	-	2.1-5.4
[39]	32 X 25	3.1-10.6	Multi section Slit	<-20	<0.005	-	-
[40]	50 X 80	4.183-6.584	Yagi based loop	≈-17	<0.0568	-	>6
[41]	40 X 50	2.5-11.0	Carbon black film coating	<-15	<0.02	-	>2.11
[42] version1	29.5 X 60	2.7-20	Stub	<-23	<0.001	0.23-0.325	-
[42] version2	29.5 X 60	3.1-20	Stub	<-20	<0.001	0.23-0.325	-
This work	18 X 36	4.83 -8.35	Stub	<25.5	<0.001	<0.33	1.6 -4.9

VI. CONCLUSION

In conclusion, our investigation into the compact eye-shaped slot antenna for MIMO UWB applications has yielded promising results. The antenna boasts a wide impedance bandwidth, excellent isolation, omnidirectional radiation characteristics, and strong MIMO performance. These attributes position it as a highly suitable candidate for use in a variety of MIMO UWB applications, emphasizing its potential impact on modern wireless communication systems.

REFERENCES

[1] Federal Communications Commission. (2002). Federal Communications Commission revision of Part 15 of the commission's rules regarding ultra-wideband transmission systems. FCC, Washington, DC, First Report and Order FCC,02.V48
URL:https://www.fcc.gov/document/revision-part-15-commissions-rules-regarding-ultra-wideband-7

[2] Sturm, C., Porebska, M., Timmermann, J., &Wiesbeck, W. (2007,September) Investigations on the applicability of diversity techniques in ultra-wideband radio 2007 International Conference on Electromagnetics in Advanced Applications (pp.899-902) IEEE.
URL:https://ieeexplore.ieee.org/document/4387450

[3] Rajagopalan,A., Gupta,G., Konanur, A.S., Hughes,B., & Lazzi G. (2007). Increasing channel capacity of an ultrawideband MIMO system using vector antennas. IEEE Transactions on Antennas and Propagation, 55(10), 2880–2887.
URL:https://ieeexplore.ieee.org/document/4339587

[4] Ben, I. M., Talbi, L., Nedil, M., &Hettak, K. (2012). MIMO- UWB channel characterization within an underground mine gallery. IEEE Transactions on Antennas and Propagation, 60(10), 4866–4874.
URL:https://ieeexplore.ieee.org/document/6236025

[5] Lee, J. M., Kim, K. B., Ryu, H. K., & Woo, J. M. (2012). A compact ultra-wideband MIMO antenna with WLAN band-rejected operation for mobile devices. IEEE Antennas Wireless Propagation Letter,11,990–993.
URL:https://ieeexplore.ieee.org/document/6276226

[6] Hong, S., Chung, K., Lee, J., Jung, S., Lee, S. S., & Choi, J.(2008). Design of a diversity antenna with stubs for UWB applications. Microwave and Optical Technology Letters, 50(5),1352–1356.
URL:https://onlinelibrary.wiley.com/doi/abs/10.1002/mop.23389

[7] Zhang, S., Ying, Z. N., Xiong, J., & He, S. L. (2009). Ultra-wideband MIMO/diversity antennas with a tree-like structure to enhance wideband isolation. IEEE Antennas Wireless Propagation Letter,8,1279–1282.
URL:https://ieeexplore.ieee.org/document/5340578

[8] See, T. S. P., & Chen, Z. N. (2009). An ultra-wideband diversity antenna. IEEE Trans. Antennas Propagation.,57(6),1597–1605.
URL:https://ieeexplore.ieee.org/abstract/document/5062526

[9] Pouyanfar, N., Ghobadi, C., Nourinia, J., Pedram, K., & Majidzadeh,M.(2018).A compact multi-band MIMO antenna with high isolation for C and X bands using defected ground structure. Radio engineering,27(3),686–693.
URL:https://www.radioeng.cz/fulltexts/2018/18_03_0686_0693.pdf

[10] Liu, P., Sun, D., Wang, P., & Gao, P. (2018). Design of a dual-band MIMO antenna with high isolation for WLAN applications. Progress In Electromagnetics Research Letters,74,23–30.
URL:https://www.jpier.org/issues/volume.html?paper=18011004

[11] Tao, J. (2016). Quan yuan Feng, ''Compact isolation-enhanced UWB MIMO antenna with band-notch character.'' Journal of Electromagnetic Waves and Applications, 30(16), 2206–2214.
URL:https://www.tandfonline.com/doi/abs/10.1080/09205071.2016.1217173

[12] Jaglan, N., Gupta, S. D., Thakur, E., Kumar, D., Kanaujia, B. K.,&Srivastava,S.(2018).Triple band notched mushroom and uniplanar EBG structures based UWB MIMO/Diversity antenna with enhanced wide band isolation. AEU-International Journal of Electronics and Communications, 90,36–44.
URL:https://www.sciencedirect.com/science/article/abs/pii/S1434841118304412

[13] Mewara, H. S., Jhanwar, D., Sharma, M. M., & Deegwal, J. K.(2018). A printed monopole ellipsoidal UWB antenna with four band rejection characteristics. AEU-International Journal of Electronics and Communications,83,222–232.
URL:https://www.sciencedirect.com/science/article/abs/pii/S1434841117316394

[14] Sharma, M., Dhasarathan, V., &Pateld, S. K. (2020). Truong Khang Nguyenb, "An ultra-compact four-port super wide-band MIMO antenna including mitigation of dual notched bands characteristics

designed for wireless network applications''. EU -International Journal of Electronics and Communications.
URL:https://www.sciencedirect.com/science/article/abs/pii/S1434841120303435

[15] Khorramizadeh, M., & Mohammad-Ali-Nezhad, S. (2021). Radar cross-section reduction of an UWB MIMO antenna using image theory and its equivalent circuit model. International Journal of RF and Microwave Computer-Aided Engineering.
URL:https://onlinelibrary.wiley.com/doi/abs/10.1002/mmce.22563

[16] Abdulkawi,W.M.,Malik,W.A.,Rehman,S.U.,Aziz,A.,Sheta, A. F. A., &Alkanhal, M. A. (2021). Design of a compact dual-band MIMO antenna system with high-diversity gain performance in both frequency bands. Micromachines.
URL:https://www.mdpi.com/2072-666X/12/4/383

[17] Ahmed,B.T.,Olivares,P.S.,Campos,J.L.M.,&Vazquez,F. M. (2018). (3.1–20) GHz MIMO Antennas. AEU-International Journal of Electronics and Communications, 94,348–358.
URL:https://www.sciencedirect.com/science/article/abs/pii/S1434841118310823

[18] Ahmed,B.T. ,Carreras,D.C., & Marin,E.G.(2021). Design And Implementation of super wide band triple band-notched MIMO antennas. Wireless Personal Communications,121, 2757–2778.
URL:https://link.springer.com/article/10.1007/s11277-021-08847-9

[19] Khalid, M., Naqvi, S. I., Hussain, N., Rahman, M., Mirjavadi, S.S., Khan, M. J., & Amin, Y. (2020). 4-Port MIMO antenna with defected ground structure for 5G millimeter wave applications. Electronics, 9,71.
URL:https://www.mdpi.com/2079-9292/9/1/71

[20] Wang, M., Nan, J., & Liu, J. (2021). High-isolation UWB MIMO antenna with multiplex-shaped stubs loaded between ground planes. International Journal of Antennas and Propagation, 2021,1155471.
URL:https://www.hindawi.com/journals/ijap/2021/1155471/

[21] Saleem,S.,Kumari,S.,Yadav,D., & Bhatnagar,D. (2020). A High Isolation UWB-MIMO Antenna with Dual Band Rejection Property. IEEE International Conference on Computing, Power and Communication Technologies 2020 (pp.212-216).
URL:https://ieeexplore.ieee.org/abstract/document/9231198

[22] Wang, L., Du, Z., Yang, H., Ma, R., Zhao, Y., Cui, X., & Xi, X.(2019). Compact UWB MIMO antenna with high isolation using fence-type decoupling structure. IEEE Antennas and Wireless Propagation Letters,18(8),1641–1645.
URL:https://ieeexplore.ieee.org/document/8752024

[23] Malekpour, N., & Honarvar, M. A. (2016). Design of high-isolation compact MIMO antenna for UWB application. Progress in Electromagnetics Research C,62,119–129.
URL:https://www.jpier.org/issues/volume.html?paper=15120902

[24] Ibrahim, A. A., & Ali, W. A. (2022). High isolation 4-element ACS-fed MIMO antenna with band notched feature for UWB communications. International Journal of Microwave and Wire-lessTechnologies,14(1),54–64.
URL:https://www.cambridge.org/core/journals/international-journal-of-microwave-and-wireless-technologies/article/abs/high-isolation-4element-acsfed-mimo-antenna-with-band-notched-feature-for-uwb-communications/E79290124A9A46E94851678346472513

[25] Addepalli, T., Babu Kamili, J., Kumar Bandi, K., Nella, A., &Sharma,M.(2022). Lotus flower-shaped 4/8- element MIMO antenna for 5GN77 and N78 band applications. Journal of Electromagnetic Waves and Applications.
URL:https://ideas.repec.org/a/taf/tewaxx/v36y2022i10p1404-1422.html

[26] Sharma,M., Vashist,P.C., Alsukayti,I., Goyal,N., Anand,D., & Mosavi, A. H. (2021). A wider impedance bandwidth dual filter symmetrical MIMO antenna for high-speed wideband wireless applications. Symmetry,14(1),29.
URL:https://www.mdpi.com/2073-8994/14/1/29

[27] Hadda, L., Sharma, M., Gupta, N., Kumar, S., & Singh, A. K.(2021).On-demand reconfigurable Wi MAX/WLAN UWB-X band high isolation 2 x 2 MIMO antenna for imaging applica-tions. IETE Journal of Research.
URL:https://www.tandfonline.com/doi/abs/10.1080/03772063.2021.1986153

[28] Sharma,M.,Singh,S.,&Varma,R.(2021).Computational design, analysis and characterization of beetle shaped high isolation multiple – input – multiple – output reconfigurable monopole-antenna with dual band filters for wireless applications. Wireless Personal Communications, 119(2),1029–1049.
URL:https://link.springer.com/article/10.1007/s11277-021-08248-y

[29] Sharma, M., Vashist, P. C., Ashtankar, P. S., & Mittal, S. K.(2021). Compact 29 2/49 4 tapered microstrip feed MIMO antenna configuration for high-speed wireless applications with band stop filters. International Journal of RF and Microwave Computer- Aided Engineering.
URL:https://onlinelibrary.wiley.com/doi/abs/10.1002/mmce.22500

[30] Sadasivam S, ThulasiBai, A compact ultra-wide band fractal antenna for breast cancer detection applications, Alexandria Engineering Journal, Volume 103, 2024, Pages 376-383, ISSN 1110-0168, https://doi.org/10.1016/j.aej.2024.06.018.
URL:https://www.sciencedirect.com/science/article/pii/S1110016824006057

[31] B Thyla, P.K. Jaya Soumeyaa, T. Jennifer, S. Maharishi, V. ThulasiBai, Design of UWB antenna for wireless capsule endoscopy, Materials Today: Proceedings, Volume 80, Part 2, 2023, Pages 1617-1622, ISSN 2214-7853, https://doi.org/10.1016/j.matpr.2023.02.128.
URL:https://www.sciencedirect.com/science/article/pii/S2214785323006624

[32] T. Thomas Leonid and Mary Grace Neela M. "A WSN-based maritime border alert system to protect fishermen." Multidisciplinary Journal for Applied Research in Engineering and Technology (2021): n. pag.
URL:https://www.mjaret.com/uploads/Files/1655907049MJARET-0921-0002.pdf

[33] Asmaa E. Farahat and Khalid F. A. Hussein, (2022) Quad-band Compact MIMO Antennas for 5G Mobile Communications ACES JOURNAL.
URL:https://journals.riverpublishers.com/index.php/ACES/article/view/14335

[34] Rajini A R, Dr. Ebenezer Abishek, Dr. S Ramesh, Dr. V Rajendran, Compact Printed Planar Eye Shaped Dipole Antenna for Ultra-Wideband Wireless Applications, Journal of Applied Science and Engineering, 913-918
URL:http://jase.tku.edu.tw/articles/jase-202210-25-5-0006

[35] Zhang, Q. . Feng, and M. K. . Khan, "Design of a Novel Circularly Polarized MIMO Antenna with Enhanced Isolation for Ultra-wideband Communication", ACES Journal, vol. 37, no. 05, pp. 607–618, Nov. 2022.

[36] S. Kolangiammal, L. Balaji, and G. Vairavel, "A Compact Planar Monopole UWB MIMO Antenna Design with Increased Isolation for Diversity Applications'', ACES Journal, vol. 37, no. 04, pp. 458–465, Apr. 2022.

[37] Najam,A., Duroc,Y., &Tedjni,S. (2011).UWB -MIMO antenna with novel stub structure. Progress In Electromagnetics Research C,19,245–257.
URL:https://www.jpier.org/PIERC/pier.php?paper=10121101

[38] Mondal,S., Mandal,K., & Sarkar, P.P.(2018). Design of MIMO antenna for ultra-wideband applications. IETE Journal of Research,64,497–502.
URL:https://www.tandfonline.com/doi/abs/10.1080/03772063.2016.1176540

[39] Haq, M. A. U., &Kozie, S. (2018). Ground plane alterations for design of high-isolation compact wideband MIMO antenna. IEEE Access, 6, 48978–48983.
URL:https://ieeexplore.ieee.org/document/8451888

[40] Jehangir, S. S., & Sharawi, M. S. (2017). A miniaturized UWB biplanar yagi-like MIMO antenna system. IEEE Antennas and Wireless Propagation Letters,16, 2320–2323.
URL:https://ieeexplore.ieee.org/document/7953428

[41] Lin,G.-S., Sung, C.-H., Chen,J.- L.,Chen,L.-S., & Houng, M.-P.(2017). Isolation improvement in UWB MIMO antenna system using carbon black film. IEEE Antennas and Wireless Propagation Letters,16,222–225.
URL:https://ieeexplore.ieee.org/document/7479549

[42] Bazil Taha Ahmed, Iva´nFerna´ndezRodrı´guez (2022), Compact high isolation UWB MIMO antennas. Wireless Networks 28, 1977-1999
URL:https://link.springer.com/article/10.1007/s11276-022-02951-9